Journal of Geoscience and Environment Protection, 2024, 12, 31-44
https://www.scirp.org/journal/gep
ISSN Online: 2327-4344
ISSN Print: 2327-4336

Study on Ecological Change Remote Sensing Monitoring Method Based on Elman Dynamic Recurrent Neural Network

Zhen Chen[1], Yiyang Zheng[2*]

[1]School of Earth Sciences and Resources, China University of Geosciences (Beijing), Beijing, China
[2]Mudanjiang Natural Resources Survey Center, China Geological Survey, Mudanjiang, China
Email: *czscott@126.com

How to cite this paper: Chen, Z., & Zheng, Y. Y. (2024). Study on Ecological Change Remote Sensing Monitoring Method Based on Elman Dynamic Recurrent Neural Network. *Journal of Geoscience and Environment Protection, 12,* 31-44.
https://doi.org/10.4236/gep.2024.124003

Received: March 17, 2024
Accepted: April 25, 2024
Published: April 28, 2024

Abstract

In this paper, Hailin City of Heilongjiang Province, China is taken as the research area. As an important city in Heilongjiang Province, China, the sustainable development of its ecological environment is related to the opening up, economic prosperity and social stability of Northeast China. In this paper, the remote sensing ecological index (RSEI) of Hailin City in recent 20 years was calculated by using Landsat 5/8/9 series satellite images, and the temporal and spatial changes of the ecological environment in Hailin City were further analyzed and the influencing factors were discussed. From 2003 to 2023, the mean value of RSEI in Hailin City decreased and increased, and the ecological environment decreased slightly as a whole. RSEI declined most significantly from 2003 to 2008, and it increased from 2008 to 2013, decreased from 2013 to 2018, and increased from 2018 to 2023 again, with higher RSEI value in the south and lower RSEI value in the northwest. It is suggested to appropriately increase vegetation coverage in the northwest to improve ecological quality. As a result, the predicted value of Elman dynamic recurrent neural network model is consistent with the change trend of the mean value, and the prediction error converges quickly, which can accurately predict the ecological environment quality in the future study area.

Keywords

Remote Sensing Ecological Index, Long Time Series, Space-Time Change, Elman Dynamic Recurrent Neural Network

1. Introduction

Using remote sensing technology to monitor the distribution and change of

ecological environment quality plays an important role in ecological environment protection. The earth's ecosystem provides a very important material basis for human production and life (Peng et al., 2015), and it also affects the physical and mental health of residents, the progress of social civilization and the long-term stability of economic development (Atasoy, 2018). Accurate and rapid monitoring, evaluation and analysis of ecological environment can provide important and reliable scientific decision-making basis for urban planning and green development (Jiang et al., 2021).

The development of remote sensing technology has made the study of long time series earth observation a reality (Wu et al., 2020; Li et al., 2021; Khare et al., 2019). Using multi-temporal remote sensing data, information such as land use type or land cover factor can be obtained to quantitatively express the characteristics of land surface dynamic change, and the rules of rapid, accurate and multi-scale analysis of land surface change can be mastered. In the practical application of long time series remote sensing monitoring, researchers often choose the same interval of 3 - 10 years for analysis (Qu et al., 2019). Due to the lack of directivity in the selection of time intervals, it is easy to miss the year of important changes. At present, the commonly used methods are artificial segmentation (Xia et al., 2019) or automatic segmentation fitting based on gradient descent method to divide the breakpoint position (Wang et al., 2017), or mathematical statistical analysis can be used to select characteristic time nodes to segment long time series.

At present, the ecological environment is mainly represented and quantified by land cover type (Qu et al., 2019) or vegetation cover index (Song et al., 2012), surface temperature (Willis et al., 2015), surface humidity (Ye et al., 2019), impervious water index (Cai et al., 2019) and other ecological indicators in the study of remote sensing data (Song et al., 2019). However, the ecological environment is a comprehensive dynamic system, and a single factor can not reflect its changes, so how to build a comprehensive evaluation index is an important scientific issue in monitoring the ecological environment quality. In recent years, there have been a variety of index mean (Wang et al., 2007) or comprehensive models constructed by area-weight method (Williams et al., 2009), and there are also comprehensive models constructed by geo-statistical methods such as coefficient of variation method (Li et al., 2020) and analytic hierarchy process (Wang et al., 2018), which are greatly affected by subjective human factors. In 2013, Xu Hanqiu (Xu, 2013) proposed a new type of Remote Sensing Ecological Index (RSEI) based on various ecological factors. Based on principal component analysis, RSEI integrated the information of four indicators, namely Dreenness, Humidity, Heat and Dryness, to comprehensively and objectively evaluate the quality of ecological environment. In recent years, the use of RSEI to monitor and evaluate ecological environments at different spatial scales has proved that the RSEI model is scalable, universal and comparable (Yue et al., 2019; Zhang et al., 2020; Hu & Xu, 2018). The selection of RSEI indicators is comprehensive, and there is a large amount of data in long-term time series research, and the data

processing is heavy (Polykretis et al., 2020; Sobrino et al., 2004).

Hailin City is rich in natural resources, and human activities mainly caused the destruction of ecological environment to a certain extent. In recent years, some researchers have studied the ecological environment of Hailin City in various aspects, but the comprehensive ecological index of Hailin City is relatively rare. Based on the remote sensing data of Hailin City from 2003 to 2023, the average RSEI index was calculated, and the temporal and spatial change characteristics of the ecological environment of Hailin City were analyzed based on the Elman dynamic recurrent neural network, which provided technical support for the ecological construction and economic and social development of Hailin City.

2. Research Area Overview and Data Preprocessing

2.1. Overview of the Study Area

Hailin City, a county-level city administered by Mudanjiang City in Heilongjiang Province, China, is located in the southeast of Heilongjiang Province and the west of Mudanjiang City, with geographical coordinates between 128˚03' - 129˚57' and 44˚02' - 45˚38'. The administrative area is 8711 square kilometers. Hailin City is located in the mid-latitude region of the northern hemisphere, belongs to the middle temperate continental monsoon climate, and the city presents obvious seasonal climate, four seasons change clearly.

The sustainable development of ecological environment in this region is related to the economic prosperity and social stability of Northeast China. The administrative diagram of the research area is shown in Figure 1.

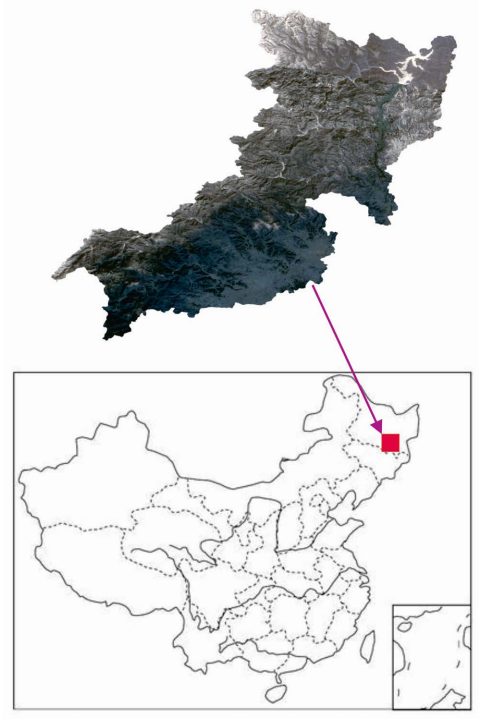

Figure 1. Study area.

2.2. Data Source and Preprocessing

Remote sensing data in the study area came from China Geospatial Data Cloud. Using radiation-corrected and atmospheric corrected Landsat 5/8/9 surface reflection data set, the cloud coverage of images from June to September was screened, and the minimum cloud coverage image of the Hailin City in recent 20 years (2003-2023) was selected. ENVI5.3, Arcgis10.7 and matlab2021 software were used to program band operations, and four indices of greenness, dryness, heat and humidity were obtained in each year. The remote sensing Ecological Index (RSEI) was obtained through principal component analysis, and the statistical analysis was carried out by ENVI5.3 and MATLAB2021 software to reach a conclusion. The technical route of this paper is shown in **Figure 2**.

3. Methods

3.1. RSEI Model

According to the remote sensing Ecological Index (RSEI) proposed by Xu Hanqiu (Xu, 2013), Normalized Difference VegetationIndex (NDVI) was selected to represent the greenness index, reflecting the vegetation growth and distribution density in the region (Song et al., 2012). Normalized Difference Soil Index, Index-based Built-up Index (IBI) and Soil Index (SI) Normalized difference soil Index, NDSI), reflects the spectral response of land desertification and urbanization (Polykretis et al., 2020). Land Surface Temperature (LST), which represents heat index (Sobrino et al., 2004), is obtained by inversion of the single-window algorithm, reflecting the heat balance of impervious water surface (Xu et al., 2015). The soil moisture content is used to reflect the land degradation (Huang et al., 2002; Baig et al., 2014). The calculation formula of each factor is as follows.

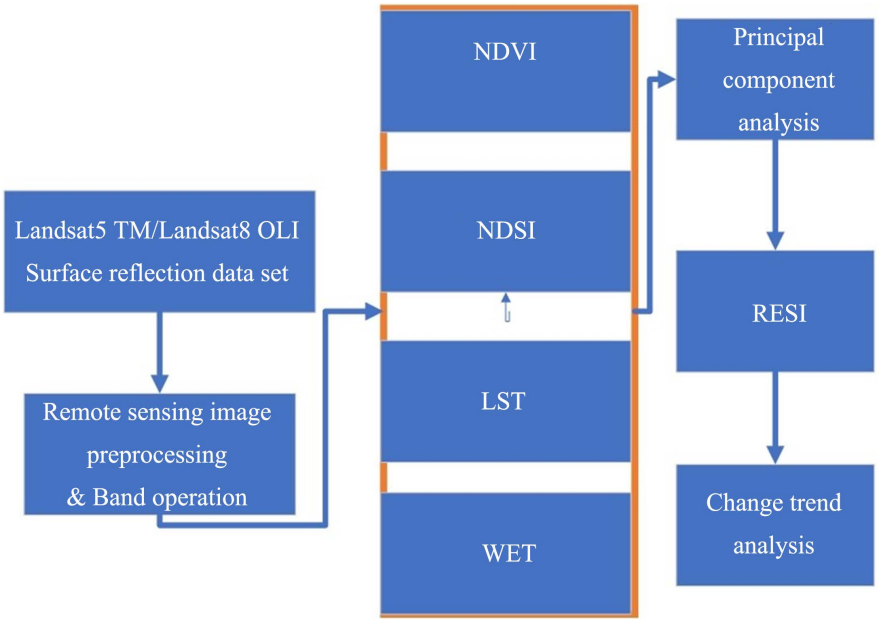

Figure 2. Technical route.

$$\mathrm{NDVI} = \frac{\rho_{NIR} - \rho_{\mathrm{red}}}{\rho_{\mathrm{NIR}} - \rho_{\mathrm{red}}} \tag{1}$$

$$\mathrm{LST} = T \Big/ \left[1 + \left(\lambda T / \rho\right) \times \ln \varepsilon\right] - 273.15 \tag{2}$$

$$\begin{aligned}\mathrm{Wet}_{\mathrm{OLI7/8}} = {} & 0.1511\rho_{\mathrm{blue}} + 0.1973\rho_{\mathrm{green}} + 0.3283\rho_{\mathrm{red}} \\ & + 0.3407\rho_{\mathrm{NIR}} - 0.7117\rho_{\mathrm{srl}} - 0.4559\rho_{\mathrm{sr2}}\end{aligned} \tag{3}$$

$$\begin{aligned}\mathrm{Wet}_{\mathrm{TM5}} = {} & 0.0315\rho_{\mathrm{blue}} + 0.2021\rho_{\mathrm{green}} + 0.3102\rho_{\mathrm{red}} \\ & + 0.1594\rho_{\mathrm{NIR}} - 0.6806\rho_{\mathrm{srl}} - 0.6109\rho_{\mathrm{sr2}}\end{aligned} \tag{4}$$

$$\mathrm{SI} = \frac{\left(\rho_{\mathrm{srl}} + \rho_{\mathrm{red}}\right) - \left(\rho_{\mathrm{blue}} + \rho_{\mathrm{NIR}}\right)}{\left(\rho_{\mathrm{srl}} + \rho_{\mathrm{red}}\right) + \left(\rho_{\mathrm{blue}} + \rho_{\mathrm{NIR}}\right)} \tag{5}$$

$$\mathrm{IBI} = \frac{2\rho_{\mathrm{srl}} \Big/ \left(\rho_{\mathrm{srl}} + \rho_{\mathrm{NIR}}\right) - \left[\rho_{\mathrm{NIR}} \Big/ \left(\rho_{\mathrm{red}} + \rho_{\mathrm{NIR}}\right) + \rho_{\mathrm{green}} \Big/ \left(\rho_{\mathrm{srl}} + \rho_{\mathrm{green}}\right)\right]}{2\rho_{\mathrm{srl}} \Big/ \left(\rho_{\mathrm{srl}} + \rho_{\mathrm{NIR}}\right) + \left[\rho_{\mathrm{NIR}} \Big/ \left(\rho_{\mathrm{red}} + \rho_{\mathrm{NIR}}\right) + \rho_{\mathrm{green}} \Big/ \left(\rho_{\mathrm{srl}} + \rho_{\mathrm{green}}\right)\right]} \tag{6}$$

$$\mathrm{NDSI} = \left(\mathrm{SI} + \mathrm{IBI}\right) \Big/ 2 \tag{7}$$

Due to the differences in numerical units and sizes of each index, it is necessary to conduct standardized processing (Xu, 2013), and then calculate the initial remote sensing ecological index (RSEI_0) through principal component analysis. The standardized formula is as follows.

$$N = \frac{I - I_{\min}}{I_{\max} - I_{\min}} \tag{8}$$

In the formula, N represents the standardized value of the indicator. I represents the value of the indicator in a certain pixel, $I_{\min}$ is the minimum value of the indicator, and $I_{\max}$ is the maximum value of the indicator. The initial remote sensing Ecological Index (RSEI_0) was calculated based on principal component analysis.

$$\mathrm{RSEI}_0 = 1 - \mathrm{PC1}\left[f\left(\mathrm{LST}, \mathrm{NDSI}, \mathrm{NDVI}, \mathrm{WET}\right)\right] \tag{9}$$

In the formula, PC1 is the first principal component. f is for standardization of indicators. In order to facilitate the measurement and comparison of indicators, RSEI_0 should also be normalized to obtain the remote sensing ecological index (RSEI), the larger the value, the better the ecological quality, and the worse the ecological quality.

3.2. Elman Dynamic Recurrent Neural Network

The basic Elman neural network consists of four layers, in addition to the input layer, hidden layer and output layer, there is a special hidden layer—the receiver layer. The acceptor layer is a delay unit, which can receive feedback signals from the hidden layer and remember the output value of the hidden layer unit at the previous time. The output of the acceptor layer is delayed and stored, and then input to the hidden layer (Liu et al., 2007). The structure of Elman's network is shown in **Figure 3**.

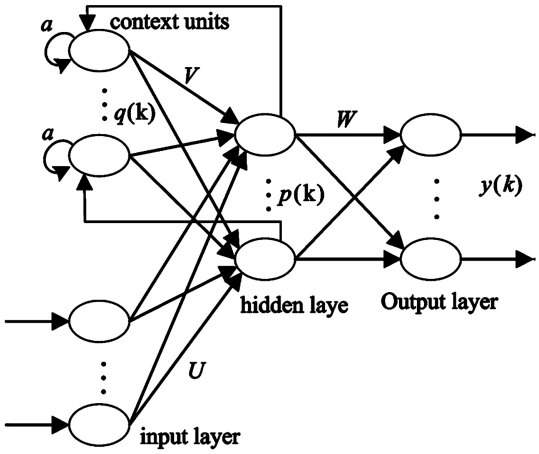

Figure 3. The schematic structure of Elman neural network (Liu et al., 2007).

Assuming that the input of the network is an I-dimensional vector x, the output of the hidden layer is an M-dimensional vector p, and the output of the inheritor layer is an M-dimensional vector q, and the output layer outputs an N-dimensional vector y. The weights of the connection between the hidden layer and the input layer, and the inheritor layer and the output layer are respectively matrix U, V, and W. Emman mathematical model of the neural network is as follows.

$$y(k) = g(Wp(k)) \tag{10}$$

$$p(k) = f(Vq(k) + Ux(k-1)) \tag{11}$$

$$q(k) = p(k-1) + aq(k-1) \tag{12}$$

In Formula (10), $g(k)$ is the activation function of the output layer element, and it takes multiple linear functions, which is the linear combination of the output of the hidden layer. In Formula (11), the $f(k)$ as the activation function of hidden layer units, much as the Sigmoid function, namely, $f(x) = 1/(1 + e - x)$. In Formula (12), a is the self-connecting feedback gain factor of the undertaking layer, and the value range is $0 \le a < 1$. When a is 0, it is the standard Elman network. When a is not 0, it is a modified Elman network. The existence of a makes the output $q(k)$ of the sublayer unit at moment k equal to the output $p(k-1)$ of the hidden layer at moment $k-1$ plus the output value $q(k-1)$ of the sublayer at moment $k-1$ A times, which can better adjust the strength of the feedback signal of the hidden layer (Ye et al., 2019; Cai et al., 2019). In this paper, the learning algorithm of Elman network adopts the ordered chain rule. The error function of the time-K system is defined as follows.

$$E(k) = \frac{1}{2}\sum_{i=1}^{n}\left(y_i(k) - d_i(k)\right)^2 \tag{13}$$

where $y_i(k)$ is the actual output of the i_{th} node, and $d_i(k)$ is the expected output of the i_{th} node. The weight W of the hidden layer of the network and the output connection changes are as follows.

$$W(k+1)=W(k)+\eta\left(-\frac{\partial E(k)}{\partial W}\right) \tag{14}$$

where η is the learning step. The same is true for weights U and V. This modified gradient descent algorithm for network weights has a slow learning rate and is easy to generate local minima. When a is 0, it is the standard Elman network. When a is not 0, it is a modified Elman network. In Figure 3, since the self-feedback gain factor a of network correction is mostly determined by trial method, the learning efficiency is higher (Song et al., 2019).

4. Results and Discussion

4.1. Results

According to the above workflow and calculation formula, using Arcgis10.7 software and matlab programming software, LST, NDSI, NDVI, WET and RESI maps of the study area from 2003 to 2023 can be obtained, as shown in Figure 4.

As can be seen from Table 1, Heat index (LST) has an overall upward trend from 2003 to 2023, a downward trend from 2003 to 2008, a continuous increase from 2008 to 2018, and a downward trend from 2018 to 2023. Dryness index (NDSI) decreased from 2003 to 2013, increased from 2013 to 2018, and decreased again from 2018 to 2023. Greenness index (NDVI) and humidity index (WET) have similar trends, increased from 2003 to 2008, decreased from 2008 to 2018, and increased from 2018 to 2023. RESI has a downward trend from 2003 to 2008, an upward trend from 2008 to 2013, a downward trend from 2013 to 2018, and an upward trend from 2018 to 2023. The overall RESI has a slight decline, and the changes of all factors related to the RESI model are shown in Figure 5.

Figure 5 shows the changes of each index and the mean value of RSEI from 2003 to 2023. The RSEI value fluctuates around 1, and RSEI decreases from 1.002 to 0.998, showing an overall downward trend. From a single index, Humidity decreased significantly from 0.514279 to 0.226924, and Dryness from 0.583503 to 0.325749, showing an upper trend. And the Heat from 0.149261 to 0.377449, showed an upward trend. It can be seen that the influence of each index on RSEI in Hailin City shows a fluctuating trend.

Table 1. LST, NDSI, NDVI, WET, RESI mean value.

Year	LST	NDSI	NDVI	WET	RESI
2003	0.149261	0.583503	0.680949	0.514279	1.001739
2008	0.089152	0.567341	0.844594	0.601247	0.989202
2013	0.134228	0.292491	0.496547	0.454595	0.993617
2018	0.705848	0.41664	0.482682	0.150253	0.987634
2023	0.377449	0.325749	0.516086	0.226924	0.998372

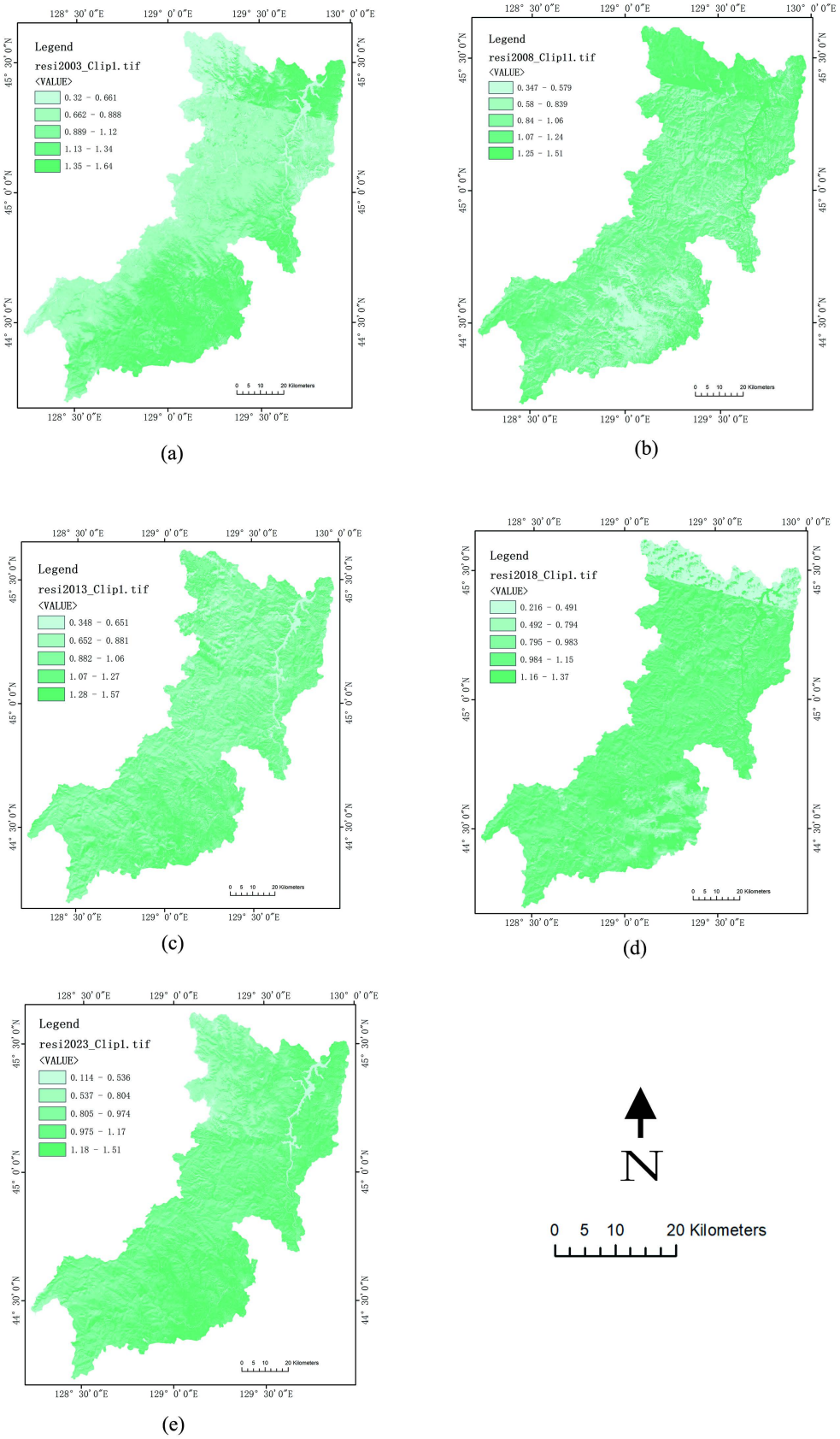

Figure 4. Remote sensing ecological index (RESI) ((a) 2003; (b) 2008; (c) 2013; (d) 2018; (e) 2023).

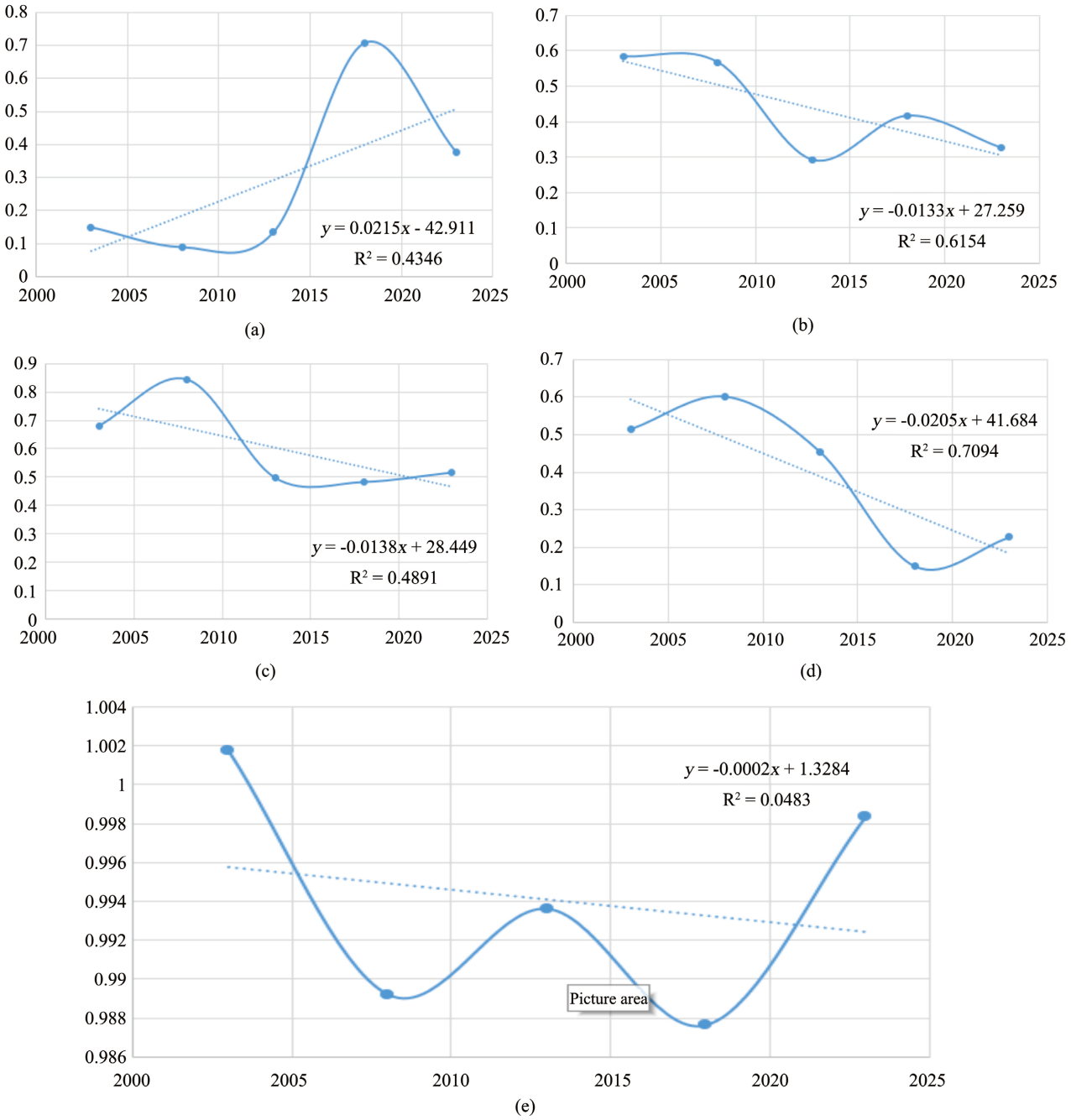

Figure 5. Trend chart ((a) LST, (b) NDSI, (c) NDVI, (d) WET, (e) RSEI).

According to the RSEI principal component analysis results of Hailin City (Table 2), it can be seen that: 1) The average contribution rate of the first principal component (PC1) is above 76.63%, indicating that PC1 has concentrated most of the characteristic information of the four indicators and it can represent the ecological environment in the region. 2) The load value of Greenness and Humidity is positive, and the load value of Dryness and Heat is negative. The higher the coincidence Greenness and Humidity, the higher the vegetation cover. The more abundant the soil moisture, and the better ecological environment

Table 2. Results of principal component analysis (Load and contribution rate of the first principal component).

Year	LST	NDSI	NDVI	WET	Contribution
2003	0.014171	−0.423720	−0.038033	0.904884	76.63%
2008	0.000421	0.208396	0.003177	−0.978039	75.38%
2013	0.028838	−0.175356	−0.223463	0.958375	66.68%
2018	−0.966731	0.218675	0.132527	0.007027	69.92%
2023	0.917816	−0.106977	−0.347640	0.159113	72.35%

quality. The higher the Dryness and Heat, the more serious natural characteristics of ecological quality reflected by soil desertification and rock exposure (Qureshi et al., 2020). 3) Compared with the change of PC1 load value, the absolute value of LST was much larger than other indicators, and the absolute sum of NDSI and LST load value was always smaller than the sum of NDVI and WET, indicating that the optimization effect of vegetation and soil moisture in Hailin was greater than the damage effect of land desertification and impervious water heat balance on the ecological environment. The RSEI index can comprehensively reflect the ecological quality of Hailin City.

In this paper, the Elman dynamic recurrent neural network selects 5 hidden node points and it uses the BP algorithm modified by momentum method to train the Elman network model. The momentum method reduces the sensitivity of the network to the local details of the error surface and effectively prevents the network from falling into local minima. In the training Elman network, the transfer function of the hidden layer element is hyperbolic tangent Sigmoid function, and the output element is linear function, and the weights and thresholds of each layer are initialized with small random numbers. The learning rate of the network is set to 0.02, the learning rate increment factor is 0.8, the learning rate reduction factor is 1.15, and the momentum constant is 0.85. In order to compare the fitting and simulation accuracy between Elman dynamic recursive network and BP network, BP network is established with the same sample data. The variable gradient backpropagation algorithm of Levenberg-Marquardt algorithm was used for training based on RSEI values from 2003 to 2023. The transfer function of the hidden layer element was hyperbolic tangent Sigmoid function, and the output element was linear function. After replacing the annual sequence (2003, 2008, 2013, 2018, 2023) with the sequence (1, 2, 3, 4, 5), the comparison between the predicted value and the expected value of the Elman test set of the ELMAN dynamic recurrent neural network is shown in Figure 6. The prediction error of the ELMAN neural network test set is shown in Figure 7.

The predicted value of Elman dynamic recurrent neural network model is consistent with the change trend of the mean value, and the prediction error converges quickly, which can accurately predict the ecological environment quality in the future study area.

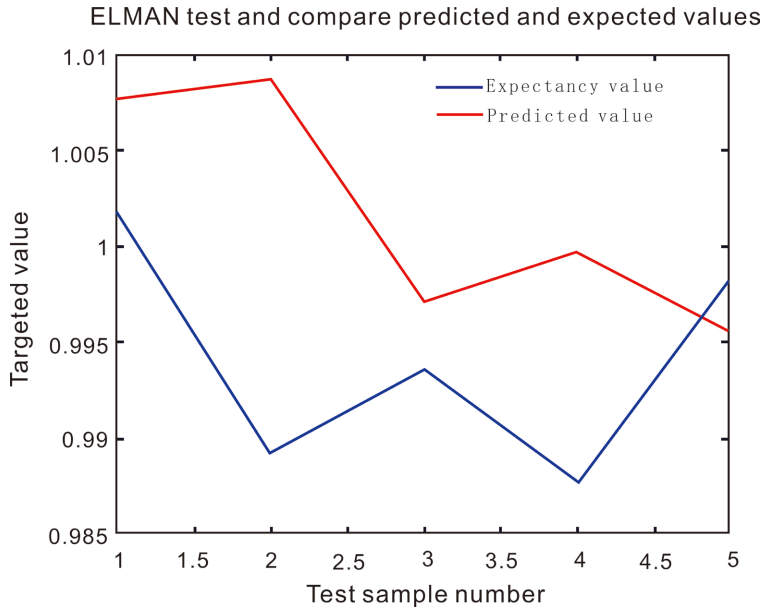

Figure 6. Comparison of predicted and expected values of the ELMAN test set.

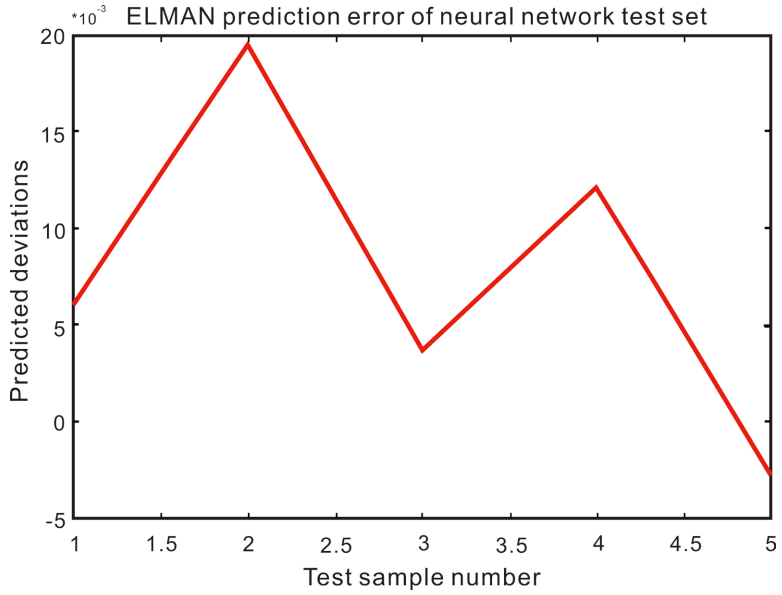

Figure 7. Prediction error of ELMAN neural network test set.

4.2. Discussion

From 2003 to 2023, the overall ecological value RSEI value showed a slight decline, mainly due to the decline of Greenness and Humidity and the rise of Heat. However, according to the changing trend of RSEI value, there is a high probability of rising in the next few years. RSEI declined most significantly from 2003 to 2008, and increased from 2008 to 2013. RSEI decreased from 2013 to 2018. RSEI increased from 2018 to 2023 again. The average RSEI has decreased slightly in the past 20 years. RSEI can effectively evaluate the ecological environment quality of Hailin City.

The expected value of RSEI of Elman dynamic recurrent neural network are consistent with the trend of RSEI mean value from 2003 to 2023, the prediction error of the model converges quickly, and the prediction effect is good. It can be proved that Elman dynamic recurrent neural network is more suitable for predicting the future ecological environment of Hailin City.

5. Conclusion

Based on long time series of remote sensing images, this study constructed the remote sensing ecological index (RSEI) of Hailin City from 2003 to 2023. The temporal and spatial visualization analysis of the ecological environment of Hailin City was carried out through the segmentation study of the time series data and combined with the trend analysis. The main conclusions are as follows.

1) From 2003 to 2023, the average contribution rate of the first principal component (PC1) of each data reached more than 76.63%. Greenness and Humidity indexes had a positive impact on the ecological environment, while dryness and heat indexes had a negative impact, which was consistent with the characteristics of the natural environment. Greenness and Humidity had the greatest impact on RSEI, and the relationship between load value and RSEI. The trend of mean value change is consistent, indicating that RSEI can comprehensively evaluate the ecological environment quality of Hailin City. The mean value of RSEI in Hailin City decreased from 1.001 to 0.998 in the past 20 years, indicating that the ecological environment of Hailin City had a trend of fluctuation and decline.

2) According to the mutation test results, the long-term time series data of Hailin City were segmented with the years 2003, 2008, 2013, 2018 and 2023 as nodes. RSEI was divided into 5 levels, and it was found that the regional distribution of remote sensing ecological index was generally good in Hailin City, mainly in the southern region.

3) Affected by different degrees of climate and human activities, the changes of ecological index in Hailin City decreased slightly with fluctuations. Significant RESI high values were concentrated in the south and northeast of Hailin City. The northwest should strengthen environmental protection and increase vegetation coverage to improve ecological quality.

Conflicts of Interest

The authors declare no conflicts of interest regarding the publication of this paper.

References

Atasoy, M. (2018). Monitoring the Urban Green Spaces and Landscape Fragmentation Using Remote Sensing: A Case Study in Osmaniye, Turkey. *Environmental Monitoring and Assessment, 190,* Article No. 713. https://doi.org/10.1007/s10661-018-7109-1

Baig, M. H. A., Zhang, L. F., Shuai, T., & Tong, Q. X. (2014). Derivation of a Tasselled Cap Transformation Based on Landsat 8 At-Satellite Reflectance. *Remote Sensing Letters, 5,* 423-431. https://doi.org/10.1080/2150704X.2014.915434

Cai, B. W., Wang, S. G., Wang, L., & Shao, Z. F. (2019). Extraction of Urban Impervious Surface from High-Resolution Remote Sensing Imagery Based on Deep Learning. *Journal of Geo-Information Science, 21,* 1420-1429.

Hu, X. S., & Xu, H. Q. (2018). A New Remote Sensing Index for Assessing the Spatial Heterogeneity in Urban Ecological Quality: A Case from Fuzhou City, China. *Ecological Indicators, 89,* 11-21. https://doi.org/10.1016/j.ecolind.2018.02.006

Huang, C. Q., Wylie, B. K., Yang, L. M., Homer, C., & Zylstra, G. (2002). Derivation of a Tasselled Cap Transformation Based on Landsat 7 At-Satellite Reflectance. *International Journal of Remote Sensing, 23,* 1741-1748. https://doi.org/10.1080/01431160110106113

Jiang, F., Zhang, Y. Q., Li, J. Y., & Sun, Z. Y. (2021). Research on Remote Sensing Ecological Environmental Assessment Method Optimized by Regional Scale. *Environmental Science and Pollution Research, 28,* 68174-68187. https://doi.org/10.1007/s11356-021-15262-x

Khare, S., Drolet, G., Sylvain, J. D., Pare, M. C., & Rossi, S. (2019). Assessment of Spatio-Temporal Patterns of Black Spruce Bud Phenology across Quebec Based on MODIS-NDVI Time Series and Field Observations. *Remote Sensing, 11,* Article 2745. https://doi.org/10.3390/rs11232745

Li, J., Huang, Y., Liu, Z.-X., Ou, D.-P., & Tan, K. (2020). Assessment of Ecological Environment Quality in Xuzhou Urban Area Based on High-Resolution Remote Sensing Images. *Modern Surveying and Mapping, 43,* 36-39.

Li, J., Sang, X., Zhang, C., Zhao, W., Liu, X., Wang, H., Wang, J., Li, J., & Yang, Y. (2021). Analysis of Long-Term Soil Water Content Change in Resource-Based Cities—A Case Study of Xilin Hot City. *Bulletin of Surveying and Mapping, No. 7,* 17-22, 38-38.

Liu, Y., Feng, Z., & Du, P. (2007). Application of Dynamic Recurrent Neural Networks in Tree Growth Prediction. *Journal of Beijing Forestry University, 29,* 99-103.

Peng, J., Dang, W., Liu, Y., Zong, M., & Hu, X. (2015). Research Progress and Prospect of Landscape Ecological Risk Assessment. *Acta Geographica Sinica, 70,* 664-677.

Polykretis, C., Grillakis, M. G., & Alexakis, D. D. (2020). Exploring the Impact of Various Spectral Indices on Land Cover Change Detection Using Change Vector Analysis: A Case Study of Crete Island, Greece. *Remote Sensing, 12,* Article 319. https://doi.org/10.3390/rs12020319

Qu, L., Liu, Y., Zhou, Y., & Li, Y. (2019). Spatial and Temporal Evolution of Ecological Land and Its Response to Ecosystem Service Function in Luoxiao Mountain Area: A Case Study of Jinggang Mountain. *Acta Ecologica Sinica, 39,* 3468-3481.

Qureshi, S., Alavipanah, S. K., Konyushkova, M., Mijani, N., Fathololomi, S., Firozjaei, M. K. et al. (2020). A Remotely Sensed Assessment of Surface Ecological Change over the Gomishan Wetland, Iran. *Remote Sensing, 12,* Article 2989. https://doi.org/10.3390/rs12182989

Sobrino, J. A., Jimenez-Munoz, J. C., & Paolini, L. (2004). Land Surface Temperature Retrieval from LANDSAT TM 5. *Remote Sensing of Environment, 90,* 434-440. https://doi.org/10.1016/j.rse.2004.02.003

Song, C. Q., Huang, B., & You, S. C. (2012). Comparison of Three Time-Series NDVI Reconstruction Methods Based on TIMESAT. In *International Geoscience and Remote Sensing Symposium (IGARSS)* (pp. 2225-2228). IEEE. https://doi.org/10.1109/IGARSS.2012.6351057

Song, L. L., Yuan, L., & Guo, C. (2019). Spatial and Temporal Pattern Analysis of Impervious Surface in Erhai Basin under the Background of Rapid Urbanization from 2005 to 2017. *Science Technology and Engineering, 19,* 336-343.

Wang, F., Wang, D., Zhang, L., Liu, J., Hu, B., Sun, Z., & Chen, J. (2018). Spatial and

Temporal Changes of Ecological Risk of Land Use in Beijing-Tianjin-Hebei City Cluster. *Acta Ecologica Sinica, 38,* 4307-4316.

Wang, Y., Zhao, Y., & Wu, J. (2017). Long-Term Dynamic Monitoring of Urban Agglomeration Ecological Quality Based on Google Earth Engine Cloud Computing: A Case Study of Guangdong-Hong Kong-Macao Greater Bay Area. *Acta Ecologica Sinica, 40,* 8461-8473.

Wang, Z., Ma, H., Zhou, D., & Sha, Z. (2007). Natural Ecological Environment Assessment Supported by Rs and Gis—A Case Study of Yalong River Project Area of South-to-North Water Diversion Project. *Salt Lake Research, 15,* 1-4.

Williams, M., Longstaff, B., Buchanan, C., Llanso, R., & Dennison, W. (2009). Development and Evaluation of A Spatially-Explicit Index of Chesapeake Bay Health. *Marine Pollution Bulletin, 59,* 14-25. https://doi.org/10.1016/j.marpolbul.2008.11.018

Willis, K. S. (2015). Remote Sensing Change Detection for Ecological Monitoring in United States Protected Areas. *Biological Conservation, 182,* 233-242. https://doi.org/10.1016/j.biocon.2014.12.006

Wu, Y., Liu, T., Tong, X., Luo, Y., Duan, L., & Wang, G. (2020). Land Use Evolution Analysis of Horqin Sandy Land Based on Long Time Series Landsat Data. *Acta Ecologica Sinica, 40,* 8672-8682.

Xia, S., Zhao, Y., Xu, X., Wen, Q., Song, Y., & Cui, P. (2019). Spatiotemporal Dynamics and Driving Factors of Agricultural Carbon Emission Rate in China from 1997 to 2016. *Acta Ecologica Sinica, 39,* 7854-7865. https://doi.org/10.5846/stxb201806041258

Xu, H. (2013). Establishment and Application of Urban Remote Sensing Ecological Index. *Acta Ecologica Sinica, 33,* 7853-7862.

Xu, H. et al. (2015). Discussion on Some Problems of Land Surface Temperature Inversion Using Single-Channel Algorithm—Taking Landsat Series Data as an Example. *Journal of Wuhan University: Information Science Edition, 40,* 487-492.

Ye, L. P., Fang, L. C., Shi, Z. H., Deng, L., & Tan, W. F. (2019). Spatio-Temporal Dynamics of Soil Moisture Driven by "Grain for Green" Program on the Loess Plateau, China. *Agriculture, Ecosystems & Environment, 269,* 204-214. https://doi.org/10.1016/j.agee.2018.10.006

Yue, H., Liu, Y., Li, Y., & Lu, Y. (2019). Eco-Environmental Quality Assessment in China's 35 Major Cities Based on Remote Sensing Ecological Index. *IEEE Access, 7,* 51295-51311. https://doi.org/10.1109/ACCESS.2019.2911627

Zhang, Y., Jiang, F., Ji, M., Jiang, H., & Wang, Z. (2020). Ecological Environment Assessment at District and County Level Based on Remote Sensing Index. *Arid Zone Research, 37,* 1598-1605.